

# Period variations and long-term cyclic changes in the light curve for the very short-period K-type contact binary YZ Phe

T. Sarotsakulchai<sup>1,2,3</sup>, S.-B. Qian<sup>1,2,4,5</sup>, B. Soonthornthum<sup>3</sup>, X. Zhou<sup>1,4,5</sup>, J. Zhang<sup>1,4,5</sup>, L.-J. Li<sup>1,4,5</sup>, D. E. Reichart<sup>6</sup>, J. B. Haislip<sup>6</sup>, V. V. Kouprianov<sup>6</sup> and S. Poshyachinda<sup>3</sup>

huangbinghe@ynao.ac.cn

## ABSTRACT

YZ Phe is a very short-period contact binary (Sp.= K2 V) with an orbital period of 0.2347 days near the short period limit (0.22 d). Here we present the complete light curves in *VRI* bands, which photometric data were obtained with the 0.61-m reflector of PROMPT-8 at CTIO in Chile during June to October 2016 and August 2017. The photometric solutions were determined by using the W-D method and results reveal that YZ Phe is a W-subtype shallow contact binary ( $f = 10\%$ ,  $q(W) = 2.635$  or  $q = 0.379$  in general meaning) with the variations of size and location of spot on the more massive component, showing a strong O'Connell effect with light-curve variations and long-term magnetic activity cycles. By compiling all available eclipse times, the result shows a long-term period decrease at a rate of  $dP/dt = -1.32(\pm 0.02) \times 10^{-8} \text{ d yr}^{-1}$ , superimposed on a cyclic variation ( $A_3 = 0.0081$  days and  $P_3 = 40.76$  years). The cyclic change can be interpreted by the light-travel time effect via the presence of a cool third body. Based on photometric solutions, the third light was detected with 2% of total light in V and I bands. Those support the existence of a third body. For the long-term period change, it can be explained by mass transfer from the more massive component ( $M_2 \sim 0.74M_\odot$ ) to the less massive one ( $M_1 \sim 0.28M_\odot$ ) or plus AML via magnetic braking. With  $q < 0.4$  and long-term period decrease, all suggest that YZ Phe is on the AML-controlled state and its fill-out factor will increase as well as the system will evolve into a deeper normal contact binary.

*Subject headings:* binaries: close - binaries: eclipsing - stars: late-type - stars: evolution - stars: activity - stars: individual (YZ Phe)

---

<sup>1</sup>Yunnan Observatories, Chinese Academy of Sciences, 650216 Kunming, P.R. China

<sup>2</sup>University of Chinese Academy of Sciences, 19 A Yuquan Rd., Shijingshan, 100049 Beijing, P.R. China

<sup>3</sup>National Astronomical Research Institute of Thailand, Donkaew, Maerim, Chiang Mai 50180, Thailand

<sup>4</sup>Key Laboratory of the Structure and Evolution of Celestial Objects, Chinese Academy of Sciences, 650216 Kunming, P.R. China

<sup>5</sup>Center for Astronomical Mega-Science, Chinese Academy of Sciences, 20A Datun Rd., Chaoyang District, 100012 Beijing, P.R. China

<sup>6</sup>Department of Physics and Astronomy, University of North Carolina, CB #3255, Chapel Hill, NC 27599, USA

## 1. Introduction

Study the late evolutionary state of low-mass contact binary systems is important to understand their physical properties and stellar evolution because their formation and evolution are still an open question in astrophysics. They usually consist of K and M type stars and those K-type contact binaries have been expected to have a short period ( $P < 0.3$  d) and a few of them are very close to the short-period limit ( $P \sim 0.22$  d). This kind of binary stars are very rare, which makes them are an important system to investigate the cause of period cut-off. The explanations for contact binaries which period near the period cutoff have been widely discussed by many authors (e.g. Rucinski 1992, 2007; Stepień 2006a, 2011; Norton et al. 2011; Jiang et al. 2012). For M-type binary stars, they have been found to have minimum period below 0.22 d, e.g. M dwarf + M dwarf; white dwarf (WD) + M dwarf binaries (Drake 2014a, Qian 2015a). To date, there are numerous eclipsing binaries below the period limit have been discovered and many of them were investigate well. While the observation and investigation of K-type contact binaries are still very poor, especially the systems with period shorter than 0.3 d as explained by Bradstreet (1985). A few K-type contact binaries that have been studied e.g. CC Com ( $P \sim 0.2207$  d, Yang et al. 2009a); BM UMa ( $P \sim 0.2712$  d, Yang et al. 2009b); FY Boo ( $P \sim 0.2411$  d, Samec et al. 2011); BI Vul ( $P \sim 0.2518$  d, Qian et al. 2013); V1799 Ori ( $P \sim 0.2903$  d, Liu et al. 2014); 1SWASP J064501.21 ( $P \sim 0.2486$  d, Liu et al. 2014); V1104 Her ( $P \sim 0.2279$  d, Liu et al. 2015); NSVS 2701634 ( $P \sim 0.2447$  d, Martignoni et al. 2016). Some of short period contact binaries which very near the limit ( $P \sim 0.20 - 0.22$  d) are showing the period decreases and some are showing the period increases as found in period change measurements for 143 SuperWASP eclipsing binaries by Lohr et al. (2013). Moreover, the investigation of SuperWASP J015100.23 (Qian et al. 2015b) as a contact binary below the period limit ( $P=0.2145$  d) suggests that contact binaries below the limit are not rapidly destroyed. But in another case e.g. NSVS 925605 (Dimitrov & Kjurkchieva 2015) which exhibits high activity including strong  $H\alpha$  emission line, large cool spots and high fill-out factor (0.7) that may be a progenitor of the predicted merging. Therefore, the relation between the short period contact binaries around the period cutoff and their period changes which investigated from the SuperWASP data are still unclear. This may be because of the lack of times of light minimum which obtained only from the SuperWASP archive, it needed more long-term observations and new data from all available sources to investigate the period changes. In addition, study these targets also provide a good chance to investigate magnetic activity cycles and O’Connell effect (O’Connell 1951) that often occur on late-type stars e.g. G, K and M types which usually show strong magnetic activity and spots similar to the sun. Study the starspots from those eclipsing binaries is less difficult than in non-eclipsing binaries because their light curves will change and show a significant difference between occulted and non-occulted region during the eclipses when there is a spot or any spots appearing on one or both components. Furthermore, contact binaries are more likely to have large spots and those spots tend to be larger than the spots on the binary stars with longer orbital period (Tran et al. 2013). However, the properties of the magnetic activity are still unclear (Qian et al. 2014) and needed to be investigated.

Recently, a study of period distribution from LAMOST spectral survey of EW-type binaries by Qian et al. (2017) has shown that the typical period of EW-type binary stars is about 0.29 d. Based on the LAMOST survey, it is also found a sharp cut-off at 0.2 d in EW-type binaries which is similar to several surveys by other investigators (e.g. Paczynski et al. 2006; Drake et al. 2014b, 2017), while a publication from the Wide-field Infrared Survey Explorer (WISE) by Chen et al. (2018) reveals a minimum period of 0.19 d for EW-type binaries. Norton et al. (2011) also found 53 W UMa type binary candidates in SuperWASP data with periods close to the short-period limit. Besides, a study of the light travel time effect (LTTE) in short period eclipsing binaries (EBs) by Li et al. (2018) suggests that contact binaries with periods close to 0.22 d are commonly accompanied by relative close tertiary companions. The frequency of EBs with tertiary companions in their sample increases as the period decreases, especially contact binaries with period  $< 0.26$  d. This indicates that the low-mass and short period contact binaries should be found a cyclic change in their  $O - C$  analysis with LTTE via the presence of a third body orbiting around their host binary stars. This is in agreement with the suggestion by Qian et al. (2013, 2015a) that a third body may have driven a binary to shorter orbital periods and evolve to contact phase. Namely, the formation of low-mass contact binary is driven by AML via magnetic braking, but the timescale of the AML for this system is long. However, there are many contact binaries that have been found to have companions (e.g., D’Angelo et al. 2006; Pribulla & Rucinski 2006; Duerberk & Rucinski 2007; Rucinski et al. 2013), which are a plausible reason to explain that some W UMa type binaries were formed by Kozai cycle (e.g., Eggleton & Kiseleva 2001; Paczynski et al. 2006). Thus, the close-in companion should play an important role for the formation and evolution by removing angular momentum from the central binary via Kozai cycles (Kozai 1962) during the early dynamical interaction or late evolution which cause the binary to have a very low angular momentum and a very short initial orbital period. In this way, the initially detached binaries with period less than 1 d will fill their primaries Roche lobes with stable mass transfer and evolve toward contact configuration via AML from magnetic stellar wind as discussed by many authors (e.g., Bradstreet & Guinan 1994; Yakut & Eggleton 2005; Stepień 2006b; Qian et al. 2017; Qian et al. 2018). However, if the short period contact binaries near the period limit are likely to show the period decrease, the separation between the components is closer, they will be instability to maintain the contact configuration and with high degree of contact, ultimately the two components will merge into single rapidly rotating star like the case of V1309 Sco (e.g. Tyndenda 2011) as explained by Lohr et al. (2012). All those reasons make the short-period contact binaries with period close to 0.22 d are important targets to study their evolution as well as their additional companions with interaction in the formation and evolution to the systems.

YZ Phe (S7172) is a high galactic southern latitude contact binary, which known as a very short period binary with 0.2347 days, and it was discovered by Hoffmeister (1963). Later, photometric data were obtained by Gessner & Meinunger (1975 and 1976) with new seven times of minimum light and its determined period of 0.3052 days. In 1989, *UBVRI* photometric observations were published by Jones (1989), who determined standard magnitudes of YZ Phe for Min I and Max II. He found that the  $V - R$  and  $V - I$  colors implied a slightly later type (K2-K5) than  $B - V$

and  $U - B$  type (K0-K2). Moreover, he concluded that YZ Phe was a W-subtype contact binary and stated that the value of 0.3052 days was incorrect because the period given by Gessner & Meinunger was a 1 day alias of the true period at that epoch, 0.2338 days. At the same year, the more observations were performed by Kilkenny & Marang (1990), who transferred all data to the  $UBV(RI)_C$  standard system and they also got nine new times of minimum light. They found that the phased light curve has O’Connell effect with clearly unequal maxima and minima. By applying a phase-dispersion minimisation technique, a period of  $0.234726 \pm 0.000002$  days was derived. The other observations of YZ Phe were done at the same year by Samec et al. (1993) and the complete  $BVR_CI_C$  light curves were obtained. Their period study with four new times of minimum light revealed that its period had remained constant at 0.23472 days for over 30 years. With their early analysis, it was reported that YZ Phe was a W-subtype contact binary with a mass ratio of 0.41, a fill-out of 16% and  $\Delta T=380$  K. Furthermore, their light-curve modeling showed that there was a cool spot on the cooler component with a large  $46^\circ$  radius and a temperature factor of 0.96. Later, Samec & Terrell (1995) published new analysis results from first publication in 1993, they found that the more massive component was the cooler one. From their new light-curve modeling, it revealed that it strongly favors the presence of a large  $54^\circ$  radius superluminous region instead of a dark spot region, which usually invoked to model asymmetries on convective contact binaries. In addition, the lowest residual of the hot spot model solution with a temperature factor of 1.03, indicates that the system consists of a K3(V) primary and a K2(V) secondary component (early K spectral-type dwarfs) with a mass ratio of  $\sim 0.40$  and shallow contact with a low fill-out factor of 2%, while the temperature  $\Delta T=255$  K. Besides, new full light curve of YZ Phe in V-band was published by Irawati et al. (2013). As their preliminary results indicated that both primary and secondary minima were shifted by 0.1 phase. The shift indicated that the ephemeris they used from Kreiner (2004) is inaccurate to predict the eclipse time and the orbital period of YZ Phe has changed since the last ephemeris measurement.

In this paper, we report new results from photometric observations in V, R and I bands for YZ Phe. The orbital period changes will be investigated and the existence of a third body will be discussed. Additionally, the long-term changes in Maximum-I and Maximum-II, also the variations of Maximum-I and Maximum-II difference will be investigated.

Table 1: Coordinates of YZ Phe, the comparison, and the check stars.

Targets	name	$\alpha_{2000}$	$\delta_{2000}$	$B$	$V$	$R$	$J$	$H$	$K$
Binary star	YZ Phe	$01^{\text{h}}42^{\text{m}}25^{\text{s}}.9$	$-45^\circ 57' 03''.9$	13.91	12.96	12.10	11.321	10.765	10.708
The comparison	UCAC2 12136273	$01^{\text{h}}42^{\text{m}}24^{\text{s}}.3$	$-45^\circ 54' 06''.5$	12.35	11.72	11.61	10.465	10.132	10.096
The check	UCAC3 89-3647	$01^{\text{h}}42^{\text{m}}29^{\text{s}}.7$	$-45^\circ 52' 47''.6$	13.74	12.78	12.48	10.921	10.475	10.310

## 2. Photometric Observations

The main photometric observations of YZ Phe in  $V$ ,  $R$  and  $I$  bands were obtained from June to October 2016 and August 2017, with back illuminated Apogee F42 2048×2048 CCD photometric system, attached to the 0.61-m Cassegrain reflecting telescope of PROMPT-8<sup>1</sup> robotic telescope. The other observations were performed with PROMPT-5, by the courtesy of data from Dr. Puji Irawati (Irawati et al. 2013), in 29 and 30 September 2012. Both telescopes are located at the Cerro Tololo Inter-American Observatory (CTIO) in Chile. The web-based SKYNET client allowed us to request and retrieve image remotely via the internet. It also provided nightly calibration images, including bias, dark, and flat-field images (Layden et al. 2010). The CCD reduction and aperture photometry measurement were done with standard procedure packages of IRAF<sup>2</sup>. The details of variable stars, the comparison and check stars are listed in Table 1. The complete photometric light curves are displayed in Figure 1; the top left panel for September 2012, top right panel for July 2016, bottom left panel for September - October 2016 and bottom right panel for 18 August 2017, respectively. Additionally, we also put all light curves from PROMPT-8 together and use the differential magnitudes of the C-Ch star to check the variations in light curves as shown in Figure 2. The figure shows that the maximum-I and maximum-II of light curves vary from time to time, and the maxima-I are often lower than maxima-II as the same pattern in paper by Samec & Terrell (1995).

## 3. Magnetic activity cycles and photometric light-curve variations

According to the photometric solutions by Samec & Terrell (1995), YZ Phe showed a large O’Connell effect in the light curves which they explained as a large hot spot with  $54^\circ$  on the cooler and more massive component of the system. How the large hot spot happened on the contact binary system is still unknown. In addition, Figure 2 shows the light curve variations with time and the largest difference between max-I and max-II is from the light curves in July 2016 with value close to 0.06 mag where max-I is the lowest and max-II is the highest. While, max-I and max-II in light curves of August 2017 is not much difference and max-I is still clearly lower than max-II. Therefore, we compile all photometric data of YZ Phe from other archives including the All-Sky Automated Survey (ASAS; Pojmanski 1997, 2002), the Siding Spring Surveys (SSS; Drake et al. 2017), the SuperWide Angle Search for Planets (SuperWASP; Pollacco et al. 2006), as well as our data from PROMPT-5 and PROMPT-8 to analyse their long-term variations of maximum (max-I and max II) as shown in Figure 3 and then we put all archives and our data together as the same scale to compare each other as displayed in Figure 4. The figure shows clearly a long-term

---

<sup>1</sup>PROMPT-8 is the Thai Southern Hemisphere Telescope (TST), operated in collaboration between National Astronomical Research Institute of Thailand (NARIT) and the University of North Carolina (UNC) at Chapel Hill in a part of the UNC-led PROMPT project, <http://skynet.unc.edu>.

<sup>2</sup>The Image Reduction and Analysis Facility (IRAF), <http://iraf.noao.edu>.

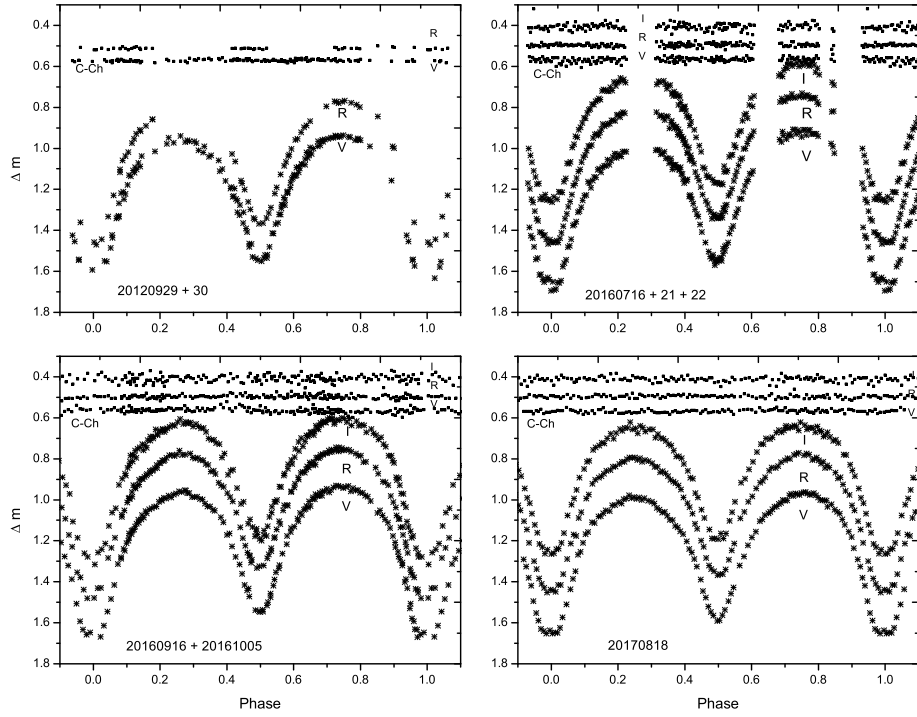


Fig. 1.— The first set of multi-color CCD light curves in V, R bands were obtained with PROMPT-5 in September 2012 (top-left panel) and the other sets in VRI bands were obtained during July, September-October 2016 and August 2017 with PROMPT-8. The differential magnitude between the comparison and the check stars (C-Ch) are stable without significant variation as shown in the figure.

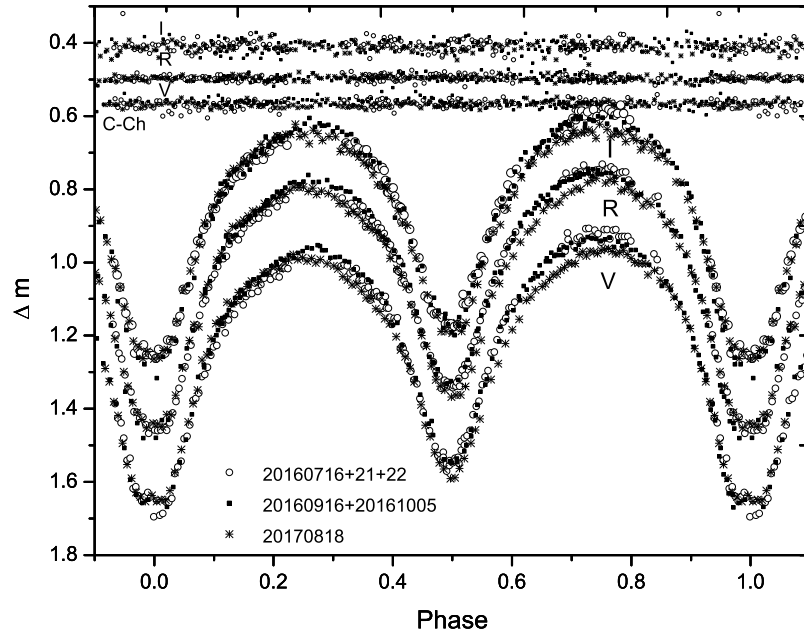


Fig. 2.— All sets of multi-color light curves from PROMPT-8 during 2016 and 2017 in Fig. 1 are put together. The differential magnitudes of the comparison and the check stars (C-Ch) are used to check the variations. The light curves show the significant variations between Max I and Max II, also Min I and Min II. It is also shown that all light curves do not overlap well, indicating that the light curve is variable.

change with sinusoidal pattern. Therefore, we use sinusoidal fitting to fit the data and it is found that the period of the long-term change is 1532.78 days (4.20 years) with a semi-amplitude of 0.06 mag. This indicates that the light curves show a long-term variation of maxima that maxima-I or maxima-II vary with time as an exact period with a maximum magnitude  $\pm 0.06$  mag or in the other words, sometimes the maximum (max-I or max II) shows a highest magnitude and sometimes it shows a lowest magnitude. This oscillation of maximum is expected to involve with changing of the size, location and type of spot (cool or hot spot) that occur on the photosphere of one or both components. Similar situations had been found in other short-period contact binaries (e.g. Kepler data), which show the variations of O’Connell effect e.g. Tran et al. (2013), Balaji et al. (2015) and Sriram et al. (2017). They found that the studies of orbital period changes with  $O - C$  curves from primary and secondary eclipse timings show an anti-correlated nature and some exhibit random walk-like variations. Those can be explained as a result of the longitudinal motions of spots and stellar differential rotations.

With the SuperWASP data of YZ Phe, we look for details in each light curve and we found the variations in them. Thus, we use least-squares method to determine each max-I and max-II in each light curve. Then, all differences between max-I and max-II (maximum I minus maximum II) are plotted with time (HJD) as the results shown in Figure 6. Our data are also put in the figure that have been done the curve fitting together. The result reveals that the differences of maximum I and maximum II vary with time as sinusoidal pattern when semi-amplitude is 0.048 mag and a period of 466.16 days (1.28 years). This may suggest that the O’Connell effect of YZ Phe shows spot activities or magnetic cycles with period of 1.28 years and average peak of  $\pm 0.048$  mag, which its period is shorter than the period of spot activity cycles of the sun (11 years). This means that the component of the contact binary is a very fast rotating star with strong magnetic activities. Sometime its max-I is dimmer than max-II (negative O’Connell effect) and sometime its max-I is brighter than max-II (positive O’Connell effect) with certain period oscillation of 1.28 years. In Figure 6, it also suggests that the O’Connell effect is variable with two stages of activity; active stage (unstable light curve) where  $\text{max-I} \neq \text{max-II}$  and inactive stage (stable light curve) where  $\text{max-I} = \text{max-II}$  as discussed by Qian et al. (2014). However, no optical flares were found during the active stage for YZ Phe. The  $H\alpha$  and Na line profiles from spectroscopic observation may help us to understand the magnetic activity on the stellar surface as the same case in EPIC 211957146 by Sriram et al. (2017). Thus, long-term observations and more photometric data, as well as spectroscopic observations are needed to confirm the results we have found in both Figure 4 and Figure 6.

#### 4. Photometric solutions with W-D method

For geometrical structure and evolutionary state of YZ Phe, the recent publication by Samec & Terrell (1995) reported that it had a large O’Connell effect appeared on light curves that also occurs on our observed light curves as displayed in Figure 1. The light curves in 2012 and July



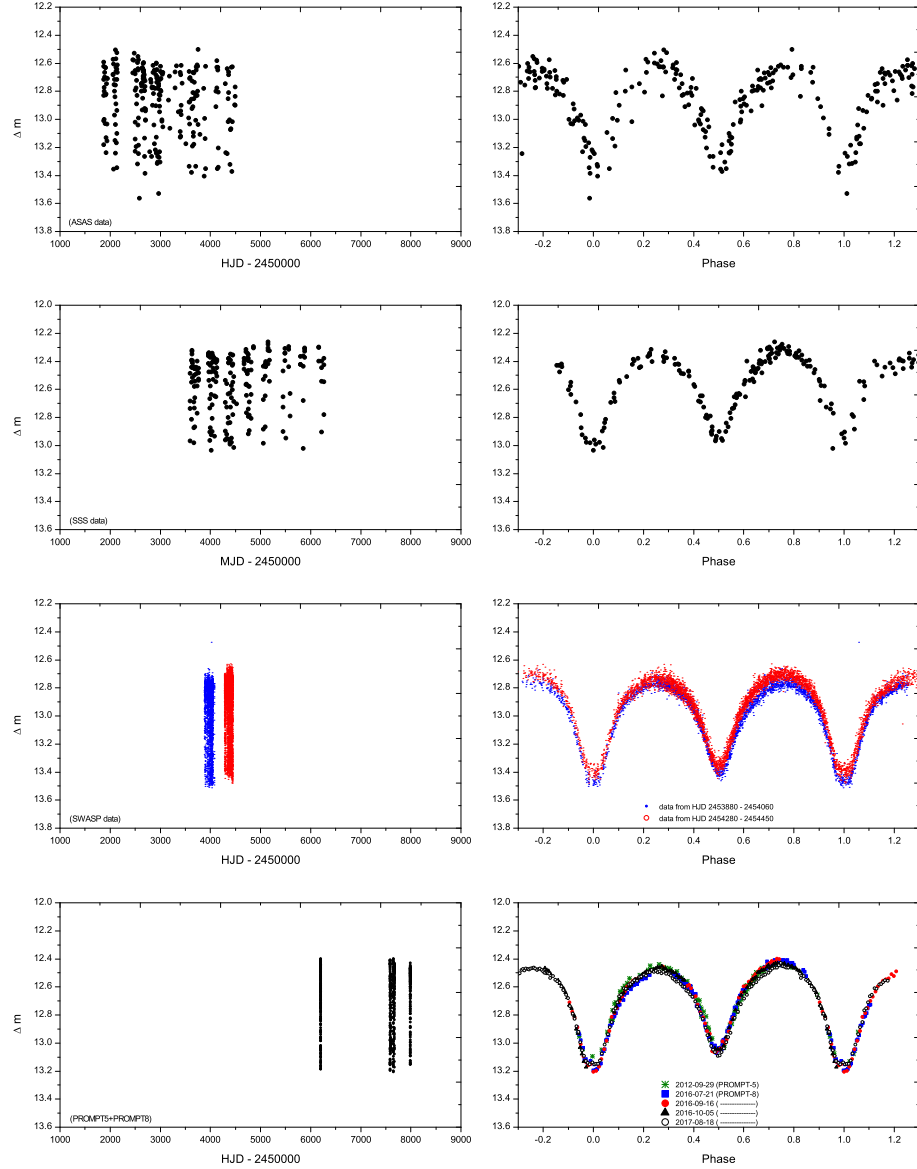


Fig. 3.— All sets of V-band light curves from ASAS (top panel), SSS (second panel), SuperWASP (third panel) archives and our observations from PROMPT-5 and PROMPT-8 are put together to check the variations of maximum. The maxima in all data of light curves in left panel show the significant long-term variations.

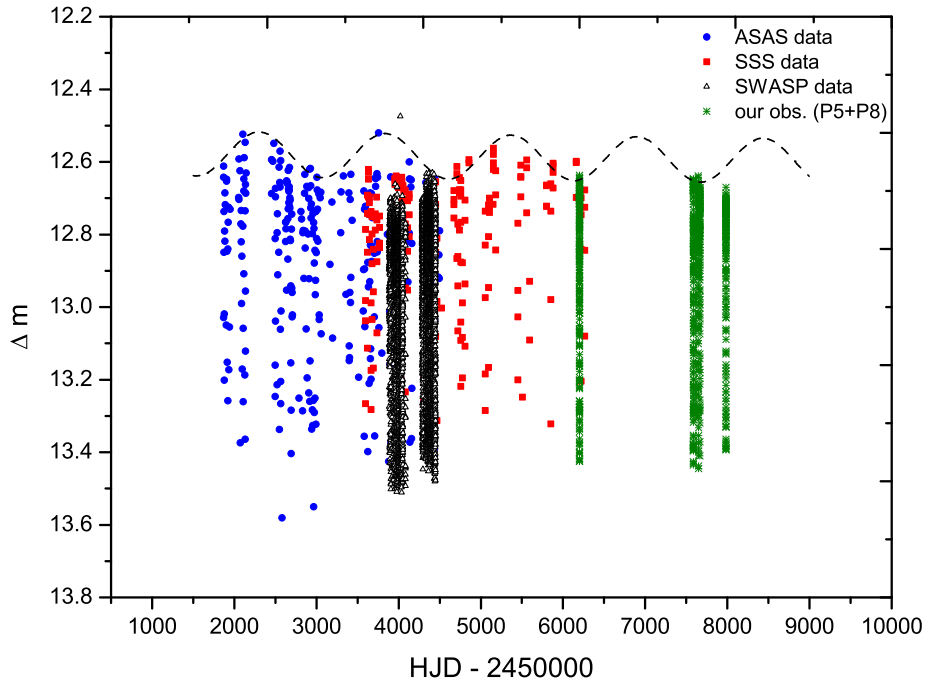


Fig. 4.— All sets of V-band light curves from Figure 3 are put together as the same scale to check the variations of maximum. The maxima of light curves show the long-term variation with sinusoidal pattern (see dashed line) of period 1532.78 days (4.20 years) and semi-amplitude 0.06 mag.

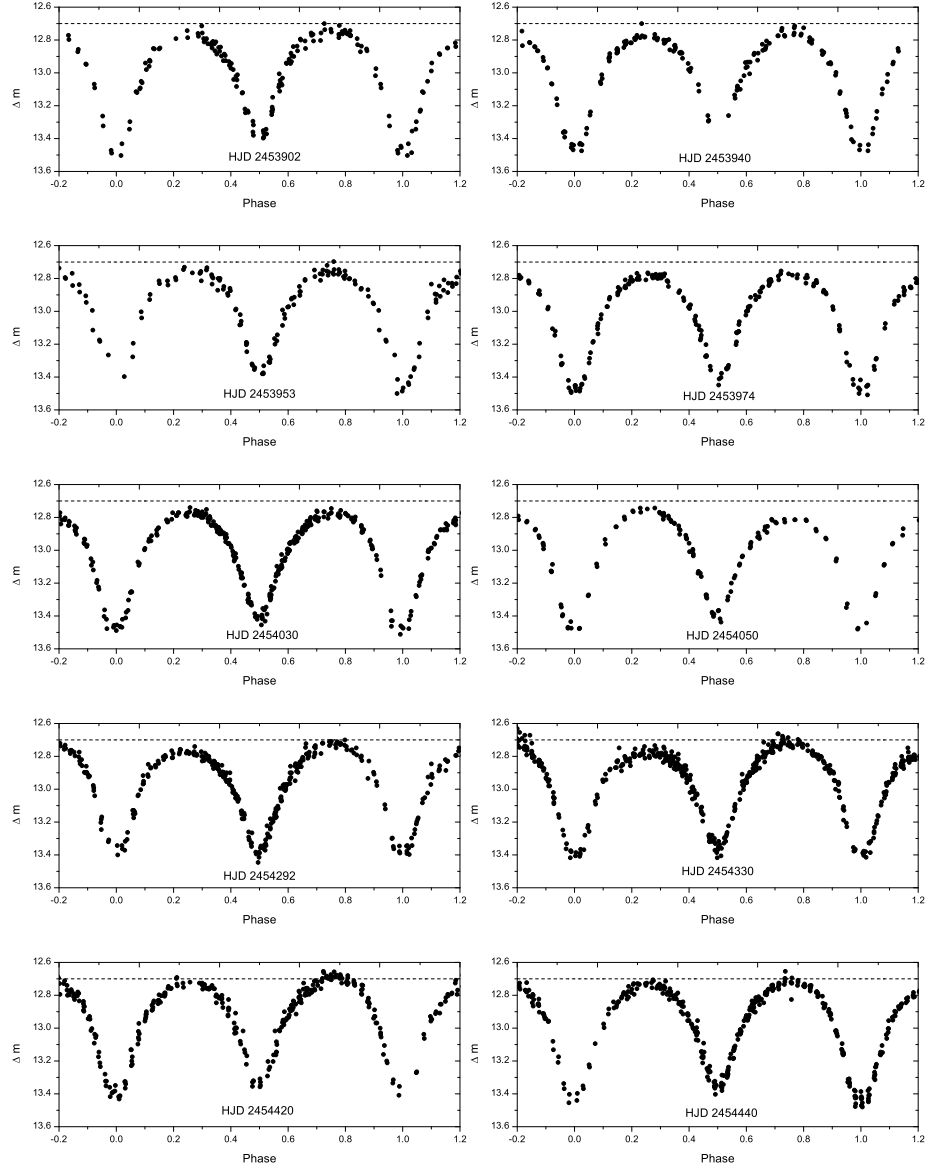


Fig. 5.— Some V-band light curves from SuperWASP archival data (2006 - 2007).

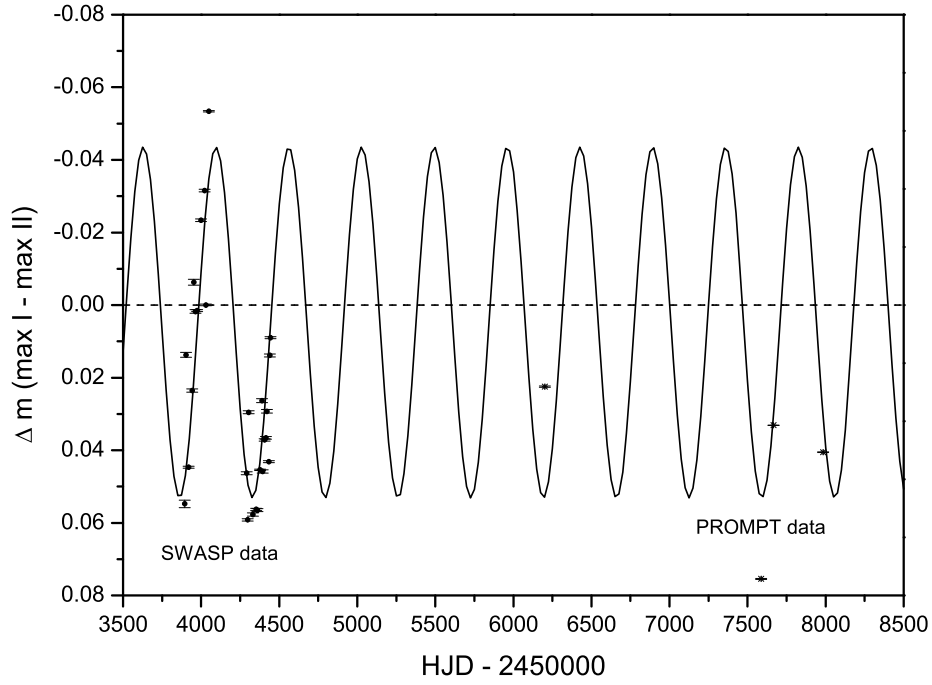


Fig. 6.— Curve fitting of the O’Connell effect for YZ Phe from SuperWASP and PROMPT data. It is shown the sinusoidal curve for the variations of maximum difference (max-I minus max-II) with a period of 466.16 days (1.28 years) and semi-amplitude of 0.048 mag. The dashed line with 0.00 mag means that max-I and max-II are equal without or less O’Connell effect.

2016 are not completed and they may not be trusted for light curves modeling. Thus, we decided to use data set that carried out in September - October 2016 and the other set in August 2017. Those data were analysed with and without spotted model by using Wilson and Devinney code (Wilson & Devinney 1971; Wilson 1990, 1994, 2012; Van Hamme & Wilson 2007) to determine their photometric elements and spot parameters. The third-light contributions are also considered in light-curve synthesis processes.

For initial input, the spectral classification from Samec & Terrell (1995) is K3 V corresponding to  $T_{eff} = 4800$  K (Cox 2000), but AAVSO database reports that  $B - V = 0.947$  which corresponds to a spectral type of K2 V (Cox 2000) and this agrees with the recent sky survey by Gaia DR2<sup>3</sup> that  $T_{eff} = 4908$  K for YZ Phe. Thus, the effective temperature of the primary star ( $T_1$ ) was fixed as 4908 K and assumed that the convective outer is already developed for both components. The bolometric albedos for star 1 and 2 were taken as  $A_1 = A_2 = 0.5$  (Rucinski 1969) and the values of the gravity-darkening coefficients  $g_1 = g_2 = 0.32$  (Lucy 1967) were used. The monochromatic and bolometric limb-darkening coefficients were chosen from Van Hamme’s table (Van Hamme 1993) by using logarithmic functions. The adjustable parameters are the inclination ( $i$ ), the mass ratio ( $q$ ), the temperature of Star 2 ( $T_2$ ), the monochromatic luminosity of Star 1 ( $L_{1V}$ ,  $L_{1R}$  and  $L_{1I}$ ), the dimensionless potential of stars 1 ( $\Omega_1 = \Omega_2$  in mode 3 for contact configuration), respectively.

In light-curve modeling, the reliable mass ratios are an important parameter and they should be obtained from precise spectroscopic radial velocity measurements. However, no spectroscopic measurements of YZ Phe were performed. Therefore, a  $q$ -search method is used to determine its initial photometric mass ratio  $q_{ph}$  and the mass ratio is set as an adjustable parameter to get a better fit later. Figure 1 indicates that YZ Phe is a W-subtype contact system which its mass ratio  $q$  is more than 1.0 ( $q(W) > 1.0$  or  $0 < 1/q < 1.0$ ) where the more massive star is cooler. During the  $q$ -search we obtained the initial mass ratio  $q = 2.8$  ( $1/q = 0.357$ ) for the first set (Sep - Oct 2016) and  $q = 2.7$  ( $1/q = 0.370$ ) for the second set (August 2017), respectively. The results from  $q$ -search method are plotted in Figure 7, the solid circles refer to the first set (Sep - Oct 2016) and open circles refer to the second set (August 2017), respectively.

Since the light curves in Figure 1 show asymmetry with a negative O’Connell effect i.e., the max-I is lower than the max-II. The other K-type contact binaries e.g., AD Cnc (Qian et al. 2007), BI Vul (Qian et al. 2013), CSTAR 038663 (Qian et al. 2014) with a deep convective envelope and fast rotation can produce a strong magnetic dynamo and solar-like activity i.e., photospheric cool spots. In this way, asymmetry in light curves can be explained as a result of spot activities. Thus, we add spot in both data sets to get a better fit. In W-D code, a spot has four parameters: the latitude ( $\theta$ ) and longitude ( $\psi$ ) of spot center in degrees, spot angular radius ( $r_s$ ) in radians

---

<sup>3</sup>This work has made use of data from the European Space Agency (ESA) mission *Gaia* (<https://www.cosmos.esa.int/gaia>), processed by the *Gaia* Data Processing and Analysis Consortium (DPAC, <https://www.cosmos.esa.int/web/gaia/dpac/consortium>). Funding for the DPAC has been provided by national institutions, in particular the institutions participating in the *Gaia* Multilateral Agreement

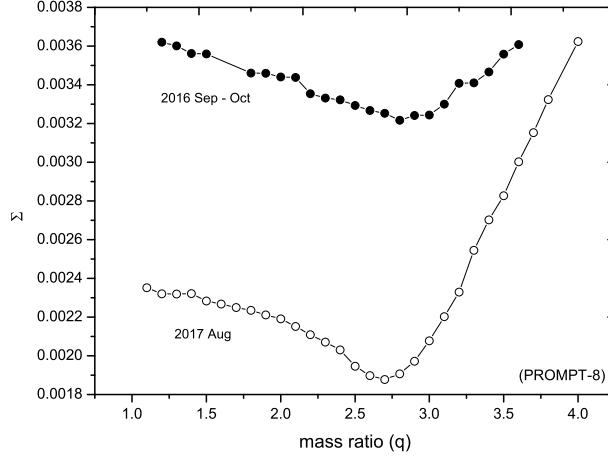


Fig. 7.— Relation Between mass ratio ( $q$ ) and the sum of weight-squares deviation ( $\Sigma$ ) for two data sets. The solutions indicate that the optimum mass ratios are in the range between 2.5 to 3.0

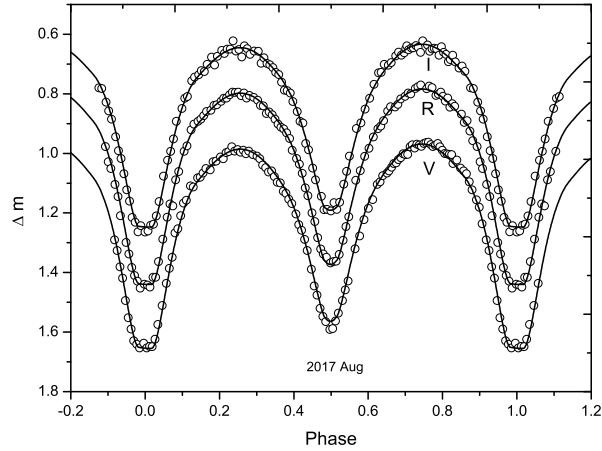


Fig. 8.— Theoretical light curves (solid lines) were computed by using W-D method compared to the observed light curves in August 2017. The results show a small difference between max-I and max-II caused by a large hot spot on the more massive component.

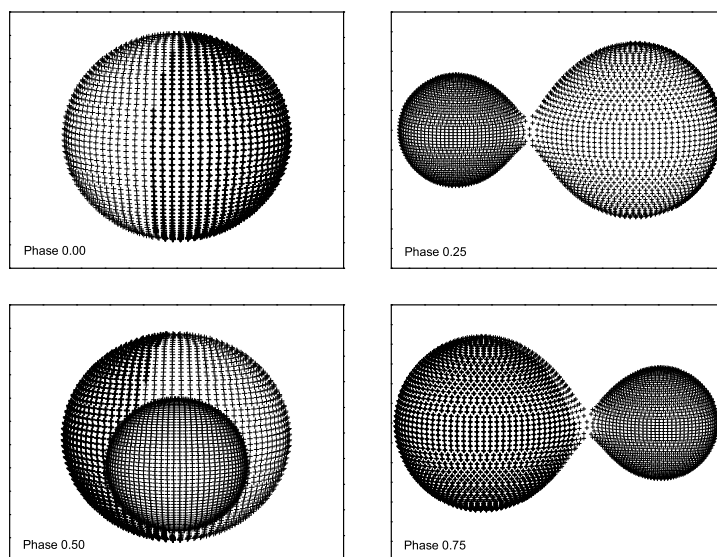


Fig. 9.— The geometrical configurations corresponding to the best-fit of photometric solutions in Figure 8 at phase of 0.00, 0.25, 0.50 and 0.75. The results show a large hot spot (89 deg) on the more massive component.

and spot temperature factor (the ratio between the spot temperature and the photosphere surface temperature of the star). In addition, we also add the third light ( $l_3$ ) as an adjustable parameter in order to get a better fit. After modeling, it is found that the third light can be detected in all bands with small values as listed in Table 2. The solutions show a large hot spot on the more massive component for the best fit in data set-2. But for data set-1, the solutions do not converge, it may be complex in light curves or because of two large spots on both stars that W-D method may not work or find the solution. Thus, the best solution for data set-1 has not obtained. The observed and the synthetic light curves are plotted in Figure 8 with their corresponding parameters listed in Table 2 and their geometrical configurations at phase of 0.00, 0.25, 0.50 and 0.75 shown in Figure 9.

### 5. Orbital period investigation

Earlier epoches and  $O - C$  data of YZ Phe were published by many authors e.g. Gessner & Meinunger (1975), Jones (1989), Kilkenny & Marang (1990), and recently by Samec & Terrell (1995). Although YZ Phe has been investigated for more than 50 years but no any variation of orbital period change was found, rather the orbital period study reported that its orbital period remained constant at 0.23472 days for over 30 years (Samec & Terrell, 1995). However, the period study of YZ Phe has been neglected for more than 20 years since last publication in 1995. Based on our photometric observations, new times of light minimum were determined and the orbital period change was re-analysed by using  $O - C$  (observed minus calculated) method. In order to re-investigate the orbital period change of YZ Phe, all available times of light minimum from the literature were compiled together with our data. The  $O - C$  data in Table 4 were recomputed with new linear ephemeris given by Kreiner (2004):

$$Min.I(HJD) = 2436765.622 + 0^d.23472665E \quad (1)$$

As the results shown in the upper panel of Figure 10, the linear ephemeris of YZ Phe is needed to be revised due to a downward parabolic pattern and a cyclic variation. To get a satisfied fit for the trend of  $(O - C)_1$  curve, it has to combine a new quadratic ephemeris with an additional sinusoidal term by assuming that the oscillation is circular ( $e = 0$ ). All times of minimum light are listed in Table 4 and the corresponding  $O - C$  curves are plotted in Fig. 10. By using a least-squares method, the new ephemeris is determined as:

$$\begin{aligned} Min.I(HJD) = & 2436765.61217(\pm 0.00038) + 0.23472754(\pm 0.00000001)E \\ & - [8.48(\pm 0.14) \times 10^{-12}]E^2 \\ & + 0.0081(\pm 0.0002) \times \sin[0^\circ.00568E + 76^\circ.549(\pm 1^\circ.238)] \end{aligned} \quad (2)$$

According to Eq. (2) and Figure 10, the sinusoidal term suggests that it has an oscillation with a period of 40.76 years and a small amplitude of cyclic variation with 0.0081 days. The  $(O - C)_2$



Table 2: Photometric solutions for 2016 and 2017 in V, R and I light curves

Parameters (models)	2016 (unspotted)	2016 (spot+l3)	2017 (unspotted)	2017 (l3)	2017 (spot+l3)
$T_1(K)$	4908	assumed	assumed	assumed	assumed
$g_1 = g_2$	0.32	assumed	assumed	assumed	assumed
$A_1 = A_2$	0.50	assumed	assumed	assumed	assumed
$q$	2.923( $\pm 0.049$ )		2.736( $\pm 0.030$ )	2.569( $\pm 0.057$ )	2.635( $\pm 0.043$ )
$T_2(K)$	4557( $\pm 9$ )		4675( $\pm 8$ )	4674( $\pm 8$ )	4658( $\pm 7$ )
$T_1 - T_2(K)$	351		233	234	250
$i(^{\circ})$	82.528( $\pm 0.453$ )		82.943( $\pm 0.358$ )	83.835( $\pm 0.555$ )	83.321( $\pm 0.346$ )
$\Omega_{in}$	2.5575		2.6067	2.6561	
$\Omega_{out}$	2.3462		2.3821	2.4181	
$\Omega_1 = \Omega_2$	6.4139( $\pm 0.0626$ )		6.2051( $\pm 0.0381$ )	5.9682( $\pm 0.0829$ )	6.0698( $\pm 0.0078$ )
$L_1/(L_1 + L_2)(V)$	0.4545( $\pm 0.0035$ )		0.3538( $\pm 0.0022$ )		
$L_1/(L_1 + L_2)(R)$	0.4362( $\pm 0.0029$ )		0.3391( $\pm 0.0019$ )		
$L_1/(L_1 + L_2)(I)$	0.4545( $\pm 0.0035$ )		0.3302( $\pm 0.0018$ )		
$L_1/(L_1 + L_2 + L_3)(V)$				0.3544( $\pm 0.0004$ )	0.3586( $\pm 0.0006$ )
$L_1/(L_1 + L_2 + L_3)(R)$				0.3461( $\pm 0.0004$ )	0.3497( $\pm 0.0005$ )
$L_1/(L_1 + L_2 + L_3)(I)$				0.3322( $\pm 0.0003$ )	0.3349( $\pm 0.0004$ )
$L_3/(L_1 + L_2 + L_3)(V)$				0.0364( $\pm 0.0024$ )	0.0233( $\pm 0.0013$ )
$L_3/(L_1 + L_2 + L_3)(R)$				0.0191( $\pm 0.0046$ )	0.0038( $\pm 0.0033$ )
$L_3/(L_1 + L_2 + L_3)(I)$				0.0333( $\pm 0.0023$ )	0.0185( $\pm 0.0012$ )
$r_1(pole)$	0.2831( $\pm 0.0014$ )		0.2805( $\pm 0.0008$ )	0.2856( $\pm 0.0023$ )	0.2829( $\pm 0.0006$ )
$r_1(side)$	0.2963( $\pm 0.0016$ )		0.2929( $\pm 0.0009$ )	0.2985( $\pm 0.0025$ )	0.2956( $\pm 0.0007$ )
$r_1(back)$	0.3358( $\pm 0.0021$ )		0.3287( $\pm 0.0012$ )	0.3349( $\pm 0.0030$ )	0.3315( $\pm 0.0012$ )
$r_2(pole)$	0.4361( $\pm 0.0052$ )		0.4421( $\pm 0.0034$ )	0.4408( $\pm 0.0076$ )	0.4413( $\pm 0.0006$ )
$r_2(side)$	0.4652( $\pm 0.0069$ )		0.4733( $\pm 0.0046$ )	0.4721( $\pm 0.0103$ )	0.4725( $\pm 0.0007$ )
$r_2(back)$	0.4896( $\pm 0.0092$ )		0.5005( $\pm 0.0062$ )	0.5008( $\pm 0.0141$ )	0.5006( $\pm 0.0009$ )
Lat(deg)					95(assumed)
Long(deg)					255(assumed)
Radius(deg)					89.185( $\pm 9.942$ )
Temp. factor					1.0041( $\pm 0.0004$ )
Spot Temp. (K)					4677( $\pm 7$ )
$f$	16.2%( $\pm 5.5\%$ )		9.8%( $\pm 3.1\%$ )	11.6%( $\pm 6.8\%$ )	9.7%( $\pm 1.3\%$ )
$\Sigma W(O - C)^2$	0.00311		0.00177	0.00149	0.00143

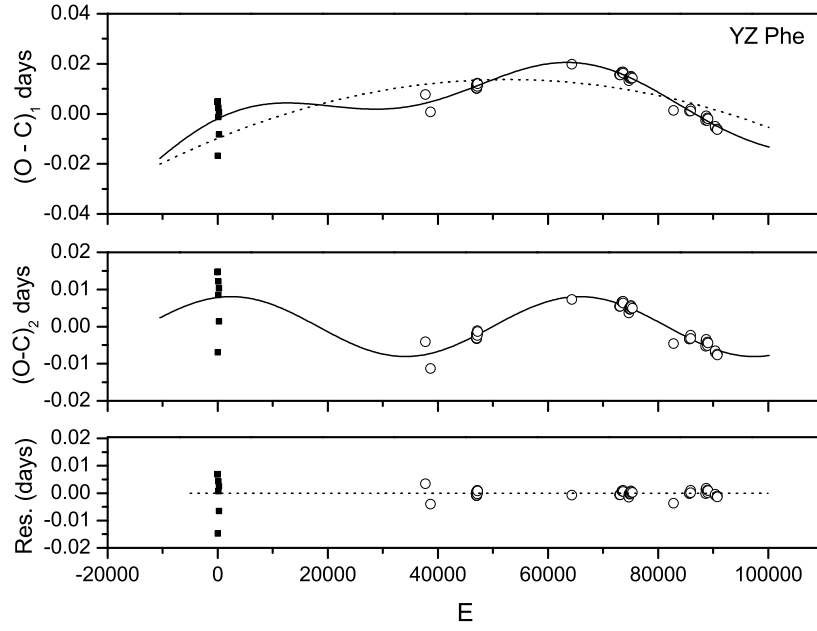


Fig. 10.— The  $(O - C)_1$  diagram in the upper panel constructed by using the linear ephemeris in Eq. (1). The solid line in the top panel refers to a combination of a long-term period decrease and a small-amplitude cyclic oscillation, while the dashed line refers to a downward parabolic curve which showing a secular period decrease. The seven dark-squared points refer to the photographic data (pg) with weight 1 and the open circles refer to the photoelectric (pe) or ccd data with weight 8, respectively.

values without the quadratic term are plotted in the middle panel and the residuals are plotted in the lowest panel of Figure 10, respectively. Although the  $(O - C)_1$  data do not cover a whole cycle and there were no eclipse timings observed between Epoch = 0 to Epoch = 40000, but most of  $O - C$  data are well constrained with the period oscillation as shown in the middle panel of Figure 10. This may suggest that the period change is reliable. The quadratic term in Eq. (2) indicates a secular period decrease at a rate of  $dP/dt = -1.32(\pm 0.02) \times 10^{-8} \text{ d yr}^{-1}$ . However, new eclipse times are needed to prove the cyclic variations.

## 6. Discussions and conclusions

Based on light curve solutions and period change analysis, we can conclude that YZ Phe is a W-subtype contact binary which the hotter component is the less massive one with mass ratio  $q = 2.635(\pm 0.043)$  and low fill-out factor  $f = 10\%$ . According to a spectral type K2 V (Gaia DR2) for the hotter component, the estimated mass of  $M_2 = 0.742M_\odot$  (Cox 2000). With the mass ratio relation, mass of  $M_1 = 0.281M_\odot$  and  $M_{total} \sim 1.02M_\odot$ . Based on the mass function of the system;  $f(m) = (M_1 + M_2) \sin^3(i)$ , where inclination  $i$  of the binary is  $83^\circ.321$ , thus the mass function of YZ Phe can be computed as  $f(m) \sim 1.02M_\odot$ . The absolute parameters of YZ Phe can be derived;  $M_1 = 0.28M_\odot$ ,  $M_2 = 0.74M_\odot$ ,  $a = 2.36R_\odot$ ,  $R_1 = 0.716R_\odot$ ,  $R_2 = 1.112R_\odot$ ,  $L_1 = 0.266L_\odot$  and  $L_2 = 0.522L_\odot$ , respectively. Our results are quite close to the parameters published by Samec (Samec & Terrell 1995) which mass ratio is close to 0.4 ( $1/q = 0.3795$  for our best-fit photometric solution) and a large hot spot on the more massive component with superluminous region (spot radius  $> 50 \text{ deg}$ ). However, we needed K1 and K2 from spectroscopic observations for  $f(m) = 1.0385 \times 10^{-7} (K1 + K2)^3 P(d)$  to determine more accurate parameters.

According to the orbital period analysis in previous section, the orbital period of YZ Phe is decreasing at a rate of  $dP/dt = -1.32(\pm 0.02) \times 10^{-8} \text{ d yr}^{-1}$  and the timescale by period decrease  $P/\dot{P} \sim 1.78 \times 10^7 \text{ yr}$ . The orbital period decrease can be explained by mass transfer or combination of mass transfer and angular momentum loss (AML) via magnetic braking. If this long term period decrease is due to the mass transfer from the more massive component to the less massive one, the transfer rate can be computed with the following equation:

$$\frac{\dot{P}}{P} = -3\dot{M}_1 \left( \frac{1}{M_1} - \frac{1}{M_2} \right) \quad (3)$$

The mass transfer rate is  $\dot{M} = 8.44 \times 10^{-9} M_\odot \text{ yr}^{-1}$  and timescale by mass transfer can be estimated as  $M_2/\dot{M} \sim 8.77 \times 10^7 \text{ yr}$  (87.7 million years) and its thermal timescale by the more massive component is  $3 \times 10^7 \text{ yr}$  (30 million years). In addition, the cyclic oscillation ( $A_3 = 0.0081$  days and  $P_3 = 40.76 \text{ yr}$ ) in orbital period analysis can be explained with the two ideas; Applegate mechanism and light-time effect via the presence of a third body. The Applegate mechanism (Applegate 1992) suggested that the cyclic changes is caused by orbital period modulation when a star goes through its magnetic activity cycle in the quadrupole moment of solar-like components.

Table 3: Times of minimum light of YZ Phe.

HJD(2400000+)	Error(days)	E	$(O - C)_1$	Method	Min	Ref.
36758.5850		-30.0	0.00480	pg	I	(1)
36764.5490		-4.5	-0.01673	pg	II	(1)
36765.6270		0.0	0.00500	pg	I	(1)
36787.4540		93.0	0.00242	pg	I	(1)
36792.4970		114.5	-0.00120	pg	II	(1)
36821.6050		238.5	0.00069	pg	II	(1)
36822.5350		242.5	-0.00821	pg	II	(1)
45621.3968	0.0002	37728.0	0.00775	pe	I	(2)
45836.7515		38645.5	0.00075	pe	II	(7)
47792.6220		46978.0	0.01144	pe	I	(3)
47793.4425		46981.5	0.01039	pe	II	(3)
47793.5610		46982.0	0.01153	pe	I	(3)
47794.6160		46986.5	0.01026	pe	II	(3)
47803.5355		47024.5	0.01015	pe	II	(3)
47807.5260		47041.5	0.01029	pe	II	(3)
47832.6428	0.0007	47148.5	0.01134	pe	II	(4)
47833.8166	0.0004	47153.5	0.01151	pe	II	(4)
47834.7557	0.0013	47157.5	0.01170	pe	II	(4)
47836.5165		47165.0	0.01205	pe	I	(3)
47836.7515	0.0005	47166.0	0.01233	pe	I	(4)
47837.3370		47168.5	0.01101	pe	II	(3)
47849.4265		47220.0	0.01209	pe	I	(3)
51868.77600		64343.5	0.01980	ccd	II	(7)
53903.61718	0.00033	73012.5	0.01564	ccd	II	(5)
53921.57367	0.00030	73089.0	0.01555	ccd	I	(5)
54000.32560	0.00024	73424.5	0.01668	ccd	II	(5)
54008.54095	0.00024	73459.5	0.01660	ccd	II	(5)
54046.33212	0.00020	73620.5	0.01679	ccd	II	(5)
54054.31236	0.00019	73654.5	0.01631	ccd	II	(5)
54294.55308	0.00018	74678.0	0.01431	ccd	I	(5)
54295.60828	0.00025	74682.5	0.01324	ccd	II	(5)
54330.58348	0.00016	74831.5	0.01417	ccd	II	(5)
54332.57907	0.00018	74840.0	0.01459	ccd	I	(5)
54353.58703	0.00027	74929.5	0.01451	ccd	II	(5)
54361.33271	0.00021	74962.5	0.01421	ccd	II	(5)
54378.58545	0.00018	75036.0	0.01455	ccd	I	(5)
54390.55707	0.00023	75087.0	0.01511	ccd	I	(5)
54391.37826	0.00029	75090.5	0.01475	ccd	II	(5)
54445.36496	0.00015	75320.5	0.01432	ccd	II	(5)
56199.69904	0.00030	82794.5	0.00142	ccd	II	(6)
56875.12470	0.00130	85672.0	0.00114	ccd	I	(7)
56878.17610	0.00110	85685.0	0.00109	ccd	I	(7)
56880.28870	0.00150	85694.0	0.00115	ccd	I	(7)
56936.62389	0.00010	85934.0	0.00195	ccd	I	(7)
56936.74038	0.00010	85934.5	0.00108	ccd	II	(7)
57567.91670	0.00010	88623.5	-0.00257	ccd	II	(6)
57585.87465	0.00010	88700.0	-0.00121	ccd	I	(6)
57591.86057	0.00020	88725.5	-0.00081	ccd	II	(6)
57647.72365	0.00020	88963.5	-0.00268	ccd	II	(6)
57647.84202	0.00020	88964.0	-0.00167	ccd	I	(6)
57666.73719	0.00007	89044.5	-0.00200	ccd	II	(6)
57983.73210	0.00016	90395.0	-0.00543	ccd	I	(6)
57983.84996	0.00011	90395.5	-0.00493	ccd	II	(6)
58069.99350	0.00080	90762.5	-0.00607	ccd	II	(7)
58070.11060	0.00020	90763.0	-0.00633	ccd	I	(7)

Notes. (1) Gessner & Meinunger 1976, (2) Jones 1989, (3) Kilkenney & Marang 1990, (4) Samec et al. 1993, (5) SWASP 2006-2007, (6) present paper, (7) <http://var.astro.cz/ocgate>.

Similar idea had been studied by Lanza & Rodono (2002), who found the correlation between magnetic modulation and orbital period variation, which is later supported by Tran et al. (2013). While the second idea about third body is supported by many evidences e.g., Liao and Qian (2010); Sriram et al. (2017) and recently by Li et al. (2018), who reported that there is a high frequency of having a third companion in contact binary when orbital period of contact binary is shorter than 0.3 d with 65% in statistical study. Their study suggests that contact binaries with periods close to the period limit 0.22 d, are commonly accompanied by relatively close third body. Furthermore, the period of cyclic change is longer with 40.76 yr, while the period of light curve variation from magnetic activity cycle in Figure 4 is just 4.2 yr, that is about 10 times. Therefore, the cyclic change in Figure 10 may be caused by light travel time effect via the presence of a third body.

W UMa variables are eclipsing contact binaries with spectral type between F and K, and orbital periods ranging from 0.2 to 1.5 days (Rucinski 1998). These late-type stars with fast rotation are expected to show high levels of chromospheric and coronal emission. However, it has no report about X-rays fluxes and radio emission observation related to YZ Phe (Beasley et al. 1993, Stepien et al. 2001, Chen et al. 2006). As our observations and archives, the light curves vary with time that may involve with spots or magnetic activities. Those suggest that spot has changed its size, location and brightness with certain period as described in section 3 e.g., Figure 4 shows a period of variations of the maximum with 4.20 yr, while Figure 6 shows the O’Connell effect with long-term magnetic activity cycles as a period of 1.28 yr that means sometimes max-I is lower than max-II (negative O’Connell effect), sometimes max-I is higher than max-II (positive O’Connell effect) and sometimes it has no light curve variation (no O’Connell effect). These O’Connell variations are caused by two stages of spot activity between active stage and inactive stage as pointed out by Qian et al. (2014). Similar situations were also found in many contact binaries e.g. BI CVn (Qian et al. 2008), CW Cas (Wang et al. 2014), GN Boo (Wang et al. 2015), EQ Tao (Li et al. 2014), AB And (Djurasevic et al. 2000), BX Peg (Lee et al. 2004, 2009), BB Peg (Kalomeni et al. 2007), AA UMa (Lee et al. 2011), V410 Aur (Luo et al. 2017) and in four recently discovered contact binaries by Djurasevic (Djurasevic et al. 2016).

Based on the photometric solutions, indicating that the light-curve modeling fit well when includes third light and spot together in modeling processes. Additionally, it has no reports about detection a third body in the system before. However, the cyclic period change in Figure 10 can be explained by light travel time effect via the presence of a third body in the system. In this case, if the third body exists and by assuming that the third body move in a circular orbit, the parameters of the third body can be computed by the mass function of a third body;

$$f(m) = (m_3 \sin i')^3 / (m_1 + m_2 + m_3)^2, \quad (4)$$

where  $f(m) = \frac{4\pi}{GP^2} \times (a'_{12} \sin i')^3$ . We also used  $a'_{12} \sin i' = A_3 \times c$ , where  $A_3$  is the amplitude of the  $O - C$  oscillation,  $c$  is the speed of light and  $i'$  is the inclination of the third body’s orbit. Thus, the mass function  $f(m) = 0.0017M_\odot$  for the tertiary, the values of the mass and the orbit radius of the tertiary can be determined. The corresponding values are displayed in Table 4.

The minimum mass of the tertiary ( $i' = 90^\circ$ ) is estimated as  $m_3 = 0.130M_\odot$  with distance  $\sim 11$  au from the central system, it may be a cool stellar companion. If the tertiary is really existent, it may play an important role for the formation and evolution of the binary system by removing angular momentum from the central binary via Kozai cycle or a combination of Kozai cycle and tidal friction, that causes the system to have an initial short orbital period (e.g. initially detached system evolves into the present contact configuration). In addition, the long-term period decrease with mass ratio  $< 0.4$  indicates that it is in agreement with Qian (Qian 2001, 2003) that this system is on AML-controlled stage and it will evolve into a deeper contact binary via magnetic stellar wind. However, no previous spectroscopic measurements were performed, all absolute parameters are estimated. Therefore, the spectroscopic observations are needed to confirm its absolute parameters and its third body, as well as its strong magnetic activities.

YZ Phe is a good target, not just to understand magnetic activity and binary evolution, but also to study the binary near the short-period limit and its third companion. New photometric and spectroscopic observations are certainly needed for further study the activity and period changes of YZ Phe in the future.

We wish to thank the Chinese Natural Science Foundation (No. 11703080) for the partly support on the research grant under the research project. And we are so grateful to referee for your comments and useful suggestions to improve the manuscript and English. This paper has made use of data from the DR1 of the WASP data (Butters et al. 2010) as provided by the WASP consortium, and the computing and storage facilities at the CERIT Scientific Cloud, reg. no CZ. 1.05/3.2.00/08.0144 which is operated by Masaryk University, Czech Republic. This research has also made use of the SIMBAD online database, operated at CDS, Strasbourg, France, NASA’s Astrophysics Data System (ADS). Finally, we would like to thank Dr. Wiphu Rujopakarn and NARIT for time allocation to use PROMPT-8 for our observations, as well as Dr. Puji Irawati for other photometric data from PROMPT-5.

Table 4: Parameters of the third body

Parameters	Value	Error	Units
$A_3$	0.0081	0.0002	days
$P_3$	40.759	0.001	years
$a'_{12} \sin i'$	1.403	0.035	AU
$f(m_3)$	0.0017	0.0001	$M_\odot$
$e_3$	0.0	assumed	-
$M_3$ ( $i' = 90^\circ$ )	0.130	0.003	$M_\odot$
$a_3$ ( $i' = 90^\circ$ )	11.0	0.4	AU

## REFERENCES

- Applegate, J. H. 1992, *ApJ*, 385, 621
- Balaji, B., Croll, B., Levine, A. M., Rappaport, S. 2015, *MNRAS*, 448, 429
- Beasley, A. J. et al. 1993, *AJ*, 106, 1656
- Bradstreet, D. H. 1985, *ApJS*, 58, 413
- Bradstreet, D. H. & Guinan, E. F. 1994, *ASP conf. Ser. (Interacting Binary stars)*, 56, 228
- Butters, O. W., West, R. G., Anderson, D. R., et al. 2010, *A&A*, 520, 10
- Chen, W. P. et al. 2006, *AJ*, 131, 990
- Chen, X.-D., Wang, S., Deng, L.-C., et al. 2018, *ApJS*, 237, 28
- Cox, A. N. 2000, *Allen’s Astrophysical Quantities* (New York: Springer)
- D’Angelo, C., van Kerkwijk, M. H. & Rucinski, S. M. 2006, *AJ*, 132, 650
- Dimitrov, D. P. & Kjurkchieva, D. P. 2015, *MNRAS*, 448, 2890
- Djurasevic, G. Rovithis-Livaniou, H., 2000, *A&A*, 364, 543
- Djurasevic, G., Essam, A., Latkovic, O., Cseki, A., et al. 2016, *AJ*, 152, 57
- Drake, A. J., Djorgovski, S. G., Catelan, M., et al. 2017, *MNRAS*, 469, 3688
- Drake, A. J., Djorgovski, S. G., Garcia-Alvarez, D., et al. 2014a, *ApJ*, 790, 157
- Drake, A. J., Graham, M. J., Djorgovski, S. G., et al. 2014b, *ApJS*, 213, 9
- Duerbeck, H. W. & Rucinski, S. M. 2007, *AJ*, 133, 169
- Eggleton, P. P. & Kiseleva, L. G. 2001, *ApJ*, 562, 1012
- Gessner, H. & Meinunger, I. 1975, *I. VSS* 8(5), 249
- Gessner, H. & Meinunger, I. 1976, *Veroff. Stern. Sonneberg* 8, 247
- Hoffmeister, C. 1963, *VSS* 6(1), 53
- Irawati, P., Sarotsakulchai, T., Suherli, J., Richichi, A., et al. 2013, *Siam Physics Congress (proceeding)*, 18
- Jiang, D.-K., Han, Z.-W., Ge, H.-W., et al. 2012, *MNRAS*, 421, 2769
- Jones, S. 1989, *IBVS*, No. 3296

- Kalomeni, B., Yakut, K., Keskin, V., et al. 2007, *AJ*, 134, 642
- Kilkenny, D. & Marang, F. 1990, *IBVS*, No. 3438
- Kozai, Y. 1962, *AJ*, 67, 591
- Kreiner, J. M., 2004, *Acta Astron.*, 54, 207
- Lanza, A. F. & Rodono, M. 2002, *AN*, 323, 424
- Layden, A. C. & Broderick, A. J. 2010, *PASP*, 122, 1000
- Lee, J. W., Kim, C.-H., Han, W.-Y., et al. 2004, *MNRAS*, 352, 1041
- Lee, J. W., Kim, S.-L., Lee, C.-U., Youn, J.-H., 2009, *PASP*, 121, 1366
- Lee, J. W., Lee, C.-U., Kim, S.-L., et al. 2011, *PASP*, 123, 34
- Li, K. et al. 2014, *AJ*, 147, 98
- Li, M. C. A., Rattenbury, N. J., Bond, I. A., et al. 2018, *MNRAS*, 480, 4557
- Liao, W.-P. & Qian, S.-B. 2010 *MNRAS*, 405, 1930
- Liu, N.-P., Qian, S.-B., Liao, W.-P., He, J.-J., et al. 2014, *RAA*, 14, 9, 1157
- Liu, N.-P., Qian, S.-B., Soonthornthum, B., Leung, K.-C., et al. 2014, *AJ*, 147, 41
- Liu, N.-P., Qian, S.-B., Soonthornthum, B., Zhu, L.-Y. et al. 2015, *AJ*, 149, 148
- Lohr, M. E., Norton, A. J., Kolb, U. C., Anderson, D. R., et al. 2012, *A&A*, 542, 124
- Lohr, M. E., Norton, A. J., Kolb, U. C., Maxted, P.F.L., et al. 2013, *A&A*, 549, 86
- Lucy, L. B. 1967, *ZA*, 65, 89
- Luo, X., Wang, K., Zhang, X.-B., Deng, L.-C., et al. 2017, *AJ*, 154, 99
- Norton, A. J., Payne, S. G., Evans, T. et al. 2011, *A&A*, 528, 90
- Martignoni, M., Acerbi, F., Barani, C. 2016, *NewA*, 46, 25
- O’Connell, D.J.K. 1951, *Riverview Pub.*, 2, 85
- Paczynski, B., Szczygiel, D. M., Pilecki, B., Pojmanski, G. 2006, *MNRAS*, 368, 1311
- Pojmanski G., 1997, *Acta Astron.*, 47, 467
- Pojmanski G., 2002, *Acta Astron.*, 52, 397
- Pollacco, D. L., Skillen, I, Collier Cameron, A., et al. 2006, *PASP*, 118, 1407



- Pribulla, T. & Rucinski, S. M. 2006, *AJ*, 131, 2986
- Qian, S.-B. 2001, *MNRAS*, 328, 635
- Qian, S.-B. 2003, *A&A*, 400, 649
- Qian, S.-B., He, J.-J., Liu, L., et al. 2008, *AJ*, 136, 2493
- Qian, S.-B., He, J.-J., Zhang, J., Zhu, L.-Y., et al. 2017, *RAA*, 17, 87
- Qian, S.-B., Jiang, L.-Q., Fernandez Lajus, E., et al. 2015a, *ApJL*, 798, 42
- Qian, S.-B., Liu, N.-P., Li, K., He, J.-J., et al. 2013, *ApJS*, 209, 13
- Qian, S.-B., Wang, J.-J., Zhu, L.-Y., et al. 2014, *ApJS*, 212, 4
- Qian, S.-B., Yuan, J.-Z., Soonthornthum, B., et al. 2007, *ApJ*, 671, 811
- Qian, S.-B., Zhang, B., Soonthornthum, B., et al. 2015b, *AJ*, 150, 117
- Qian, S.-B., Zhang, J., He, J.-J., Zhu, L.-Y., et al. 2018, *ApJS*, 235, 5
- Rucinski, S. M. 1969, *AcA*, 19, 245
- Rucinski, S. M. 1992, *AJ*, 103, 960
- Rucinski, S. M. 1998, *AJ*, 115, 1135
- Rucinski, S. M. 2007, *MNRAS*, 382, 393
- Rucinski, S. M., Pribulla, T. & Budaj, J. 2013, *AJ*, 146, 70
- Samec, R. G., et al. 1993, *IBVS*, No. 3884
- Samec, R. G. & Terrell, D. 1995, *PASP*, 107, 427
- Samec, R. G., Oliver, B., Figg, E. R., et al. 2011, *IBVS*, No. 5963
- Sriram, K., Malu, S., Choi, C. S., et al. 2017, *AJ*, 153, 231
- Stepien, K., Schmitt, J.H.M.M. & Voges, W. 2001, *A&A*, 370, 157
- Stepien, K. 2006a, *Acta Astron.*, 56, 347
- Stepien, K. 2006b, *Acta Astron.*, 56, 199
- Stepien, K. 2011, *Acta Astron.*, 61, 139
- Tran, K., Levine, A., Rappaport, S., Borkovits, T., et al. 2013, *ApJ*, 774, 81
- Tylenda, R., Hajduk, M., Kaminski, T. et al. 2011, *A&A*, 528, 114

- Van Hamme, W. 1993, AJ, 106, 2096
- Van Hamme, W. & Wilson, R. E. 2007, ApJ, 661, 1129
- Wang, J. J. et al. 2014, AJ, 148, 95
- Wang, J. J. et al. 2015, AJ, 149, 164
- Wilson, R. E. 1990, ApJ, 356, 613
- Wilson, R. E. 1994, PASP, 106, 921
- Wilson, R. E. 2012, AJ, 144, 73
- Wilson, R. E. & Devinney, E. J. 1971, ApJ, 166, 605
- Yakut, K. & Eggleton, P. P. 2005, ApJ, 629, 1055
- Yang, Y.-G., Lu, G.-L., Yin, X.-G., Zhu, C.-H., Nakajima, K. 2009a, AJ, 137, 236
- Yang, Y.-G., Wei, J.-Y., Nakajima, K. 2009b, PASJ, 61, 13